Weighted Coherent Detection of QCSP frames

Kassem Saied, Luis Enrique Camacho Flores, E. Boutillon

Weighted Coherent Detection of QCSP frames

Kassem Saied
Lab-STICC (UMR 6285)
Université Bretagne Sud
Lorient, France

Luis Camacho
Universidad Nacional de Ingeniería
INICTEL - UNI
Lima, Peru

Emmanuel Boutillon
Lab-STICC (UMR 6285)
Université Bretagne Sud
Lorient, France

***Abstract*—A new efficient preamble-less short frame, called Quasi-Cyclic Short Packet (QCSP), has been recently proposed for the Internet of Things (IoT) deployment. It has demonstrated its good performances in the process of detection, synchronization, and error correction in an asynchronous Additive White Gaussian Noise (AWGN) channel, with residual frequency offset, and at a very low Signal-to-Noise Ratio (SNR). The detection process uses the normalized score of a non-coherent frame match filter to assess the presence of a frame or not. In this paper, we improve the detection performance by combining non-coherent detection with coherent detection. The proposed method decreases the probability of miss-detection by two decades, for a given probability of false alarm.**

***Index Terms*—IoT, Short-packets, Coherent detection, Weighting factor.**

I. INTRODUCTION

Transmitting many short packets in a wide area Internet of Things (IoT) network is a complex problem. In fact, when the message length is small (temperature sensor sending data to a base station for example), information exchange related to signaling, synchronization, and identification represents a cost of radio-spectrum utilization that alleviates resources for effective data transmission. This problem introduces a fundamental change in massive IoT networks, leading to unsupervised networks [1]. Moreover, the use of a preamble associated with each frame to facilitate the detection and synchronization tasks becomes also problematic since a significant part of the bandwidth is wasted [2]. In [3]–[7], efficient methods for transmitting and receiving short packets without preamble have been demonstrated for positive SNR values (i.e., SNR greater than 0 dB, typically), but not for very noisy environments.

Recently, a new preamble-free frame, called Quasi-cyclic Short Packet (QCSP), has been proposed [8]. The QCSP frame is based on the association of a Cyclic Code Shift Keying (CCSK) modulation and a Non-Binary Forward Error Control (NB-FEC) code. It is shown that the frame can be reliably detected thanks to a simple non-coherent detection algorithm based on the comparison between a cumulative score function and a threshold value U_0. In [9], another detection method called a time-sliding window has been proposed which replaces the frequency domain correlation with a time domain correlation taking full advantage of the QCSP frame structure. In [10] and [11], time, frequency, and phase synchronization methods are proposed and show their good performances for the short-data packet transmission.

Moreover, the proposed method which is presented in [8] is based on a theoretical Gaussian channel with a calibrated level of noise and signal. In a real radio receiver, the amplitude of the signal is subjected to an unknown multiplicative factor due to the front end of the radio frequency stage in general, and the behavior of the automatic gain control in particular. Henceforth, the comparison of the score function with a fixed threshold becomes sensitive to a scaling factor, leading either to a huge number of false alarms when the multiplicative factor is greater than expected, or to a vanishing probability of detection when the multiplicative factor is lower than expected. To mitigate this problem, the signal is normalized by its energy, so the score function becomes independent of a multiplicative factor affecting the input signal. However, the drawback of this normalization is that the energy increased at a frame arrival is flattened by the normalization. This increased energy can't be used anymore to help detection, which leads to a sensitive reduction in detection performance (see section II-B).

In this paper, we first propose to replace non-coherent detection with a coherent detection method. This method is based on the frequency domain searches on the successive decoded symbols of a frame. Prior to this frequency search, the decoded symbols are weighted according to their reliability. This method is called Weighted Coherent Sum (WCS) detection. The second contribution is to combine both non-coherent detection and coherent detection techniques to further improve detection. The performance analysis of the proposed methods is performed as a trade-off between the probability of miss-detection and the probability of false alarm.

The rest of the article is structured as follows. Section II presents the QCSP communication system model and illustrates the problem statement of the article. Section III describes the proposed enhancement of the detection method in detail. The simulation results are summarized and analyzed in section IV. Finally, the conclusion and perspectives are presented in Section V.

II. DETECTION OF QCSP FRAMES

This section illustrates firstly the overall QCSP communication chain. Then, it explains the Detection Error Trade-off (DET) probabilities. Finally, it states the effect

This work has been funded by the French ANR under grant number ANR-19-CE25-0013-01 (QCSP Project: https://qcsp.univ-ubs.fr/).

of normalization on the detection performance proposed in [8].

A. QCSP Communication chain

The overall QCSP communication chain is shown in Fig. 1. Let us describe it in detail. In the following, the Galois Field of order $q = 2^p, p \in \mathbb{N}$, is represented as GF($q$). At the transmitter side, a Non-Binary Error Correction Code (NB-ECC) of coding rate $R_c = \frac{K}{N}$, encodes an input message $\boldsymbol{M}$ of K GF(q) symbols (each symbol on p bits), to N GF(q) symbols forming the codeword $\boldsymbol{C}$. The considered NB-ECC is Non-Binary Low-Density Parity-Check (NB-LDPC) since they are efficient for small frame lengths. Consequently, the output codeword is composed by the vector $\boldsymbol{C}$ of N elements in GF(q), $\boldsymbol{C} = (c_n)_{n=0,1,...,N-1}$. In the sequel, each element of GF(q) is considered as an element in $[0, q-1]$ using its binary representation. The CCSK modulation maps each GF symbol c_n of the codeword $\boldsymbol{C}$ to a circular shift of an initial binary sequence $\boldsymbol{P}_0$ by c_n positions. Note that the sequence $\boldsymbol{P}_0$ has good auto-correlation properties. In this paper, we study only the case where the length of $\boldsymbol{P}_0$ length is set to q, defining a modulation rate of $R_m = \frac{p}{q}$. The circularly c_n-right-shifted version of $\boldsymbol{P}_0$ is denoted $\boldsymbol{P}_{c_n}$, thus, $\boldsymbol{P}_{c_n} = \boldsymbol{P}_0(i - c_n \mod q)$, $i = 0, 1, ..., q-1$.

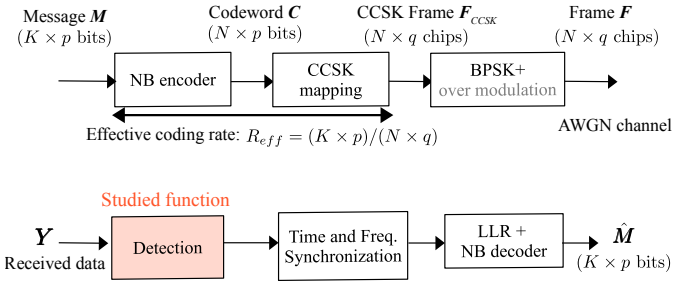

Fig. 1. QCSP System Model.

The combination of the two rates, R_m and R_c, defines the QCSP effective rate $R_{eff} = \frac{Kp}{Nq}$. Consequently, the CCSK frame $\boldsymbol{F}_{CCSK}$ is the concatenation of N encoded CCSK symbols i.e. $\boldsymbol{F}_{CCSK} = (\boldsymbol{P}_{c_n})_{n=0,1,...,N-1}$. Finally, the QCSP frame $\boldsymbol{F}$ is obtained after applying Binary Phase Shift Keying (BPSK) modulation. Moreover, to help the time synchronization process [10], an additional modulation (called Over-modulation) is used at the symbol level to generate a known pattern of phase shift. As a result of the use of over-modulation, we finally obtain the QCSP frame $\boldsymbol{F}$ defined as $\boldsymbol{F} = ((-1)^{b_n}\boldsymbol{P}_{c_n})_{n=0,1,...,N-1}$, with the sequence $\boldsymbol{B} = (b_n)_{n=0,1,...,N-1} \in \{0,1\}$ is a sequence with good auto-correlation properties. Since we are focusing on the detection process, the effect of over-modulation can be assumed as fully mitigated at the receiver side, and thus, it is no more considered in the rest of the paper.

The QCSP frame passes through a complex Additive White Gaussian Noise (AWGN) channel $\mathcal{N}(0, \sigma^2)$ of zero mean and standard deviation $\sigma = \sqrt{10^{-\mathrm{SNR}/10}}$, where SNR represents the signal-to-noise ratio E_s/N_0 of the transmission channel. Carrier frequency errors are also considered, leading to a frequency offset F Hz affecting the received frame. In T_c seconds (duration of a chip), the frequency offset generates a rotation $\frac{T_c F}{2\pi}$ radians between two consecutive chips. In the sequel, a normalized frequency offset $f_0 = FT_c$ is used. This f_0 generates a rotation of $2\pi f_0 q$ radians between two chips separated by a symbol duration $T = qT_c$. Note that f_0 can be bounded to the interval $[-f_m/2, f_m/2]$ since the detection process [8] uses a time-frequency decomposed grid with a frequency resolution of f_m. Typically, f_m should verify $f_m \leq \frac{1}{2q}$ so that, at maximum, there is less than half a rotation between the first chip and the last chip of a given symbol. This maximum rotation still allows the decoding of the symbols with a limited degradation penalty. Finally, the initial phase offset φ is unknown too and $\varphi \in [0,\ 2\pi]$. At the receiver side, the k^{th} term $y(k)$ of the received frame $\mathbf{Y}$ can be expressed as

$$y(k) = e^{j(2\pi f_0 k + \varphi)}\boldsymbol{F}(k) + z(k). \tag{1}$$

for $k = 0, 1, \ldots, qN-1$. The additive term $z(k)$ corresponds to the noise injected by the channel.

At the reception time, the received data stream $\mathbf{Y}$ is taken as a stream of N blocks $\mathbf{Y} = (\boldsymbol{y}_n)_{n=0,1,...,N-1}$, where the n^{th} bloc corresponds to the transmission of the n^{th} symbols of $\boldsymbol{F}$. In other words, $\boldsymbol{y}_n = (y(k))_{k=nq,nq+1,...,(n+1)q-1}$, or directly, $\boldsymbol{y}_n(l) = y(qn+l)$, $l = 0, 1, \ldots, q-1$. According to (1) The value of $\boldsymbol{y}_n(l)$ is thus equal to

$$\boldsymbol{y}_n(l) = e^{j(2\pi f_0(nq+l)+\varphi)}\boldsymbol{P}_0(l - c_n) + z(nq+l), \tag{2}$$

The key to the detection method is obtaining a reliable score function that takes high values when a QCSP frame is presented and low values when the QCSP frame is absent.

Each received QCSP frame $\mathbf{Y}$ is demodulated by correlating $\boldsymbol{y}_n$ with each of the q possible shifted sequences $\boldsymbol{P}_s$, $s = 0, 1, ..., q-1$ to generate the vector $\boldsymbol{L}_n = (L_n(s))_{s=0,1,...,q-1}$ where the s^{th} component is defined as

$$L_n(s) = \sum_{l=0}^{q-1} y_n(l)\boldsymbol{P}_s(l) \tag{3}$$

The vector $\boldsymbol{L}_n$ is equal to the circular correlation of $\boldsymbol{y}_n$ and $\boldsymbol{P}_0$, i.e.,

$$\boldsymbol{L}_n = \boldsymbol{y}_n \star \boldsymbol{P}_0. \tag{4}$$

where $\star$ denotes the circular correlation. This computation can thus be done in the spectral domain as

$$\boldsymbol{L}_n = \mathcal{F}^{-1}(\mathcal{F}(\boldsymbol{y}_n) \odot \mathcal{F}(\boldsymbol{P}_0)^*), \tag{5}$$

where the operator $\odot$ denotes the element-wise (or Hadamard) product of two vectors, and $\mathbf{X}^*$ represents the vector obtained by taking the conjugate of each component of $\mathbf{X}$. The operators $\mathcal{F}$ and $\mathcal{F}^{-1}$ represent the Fast Fourier Transform (FFT) and its inverse (IFFT), respectively.

The maximum likelihood decision d_n at the symbol is given as

$$d_n = \underset{s=0,1,...,q-1}{\arg\max}\ \{|L_n(s)|\},$$

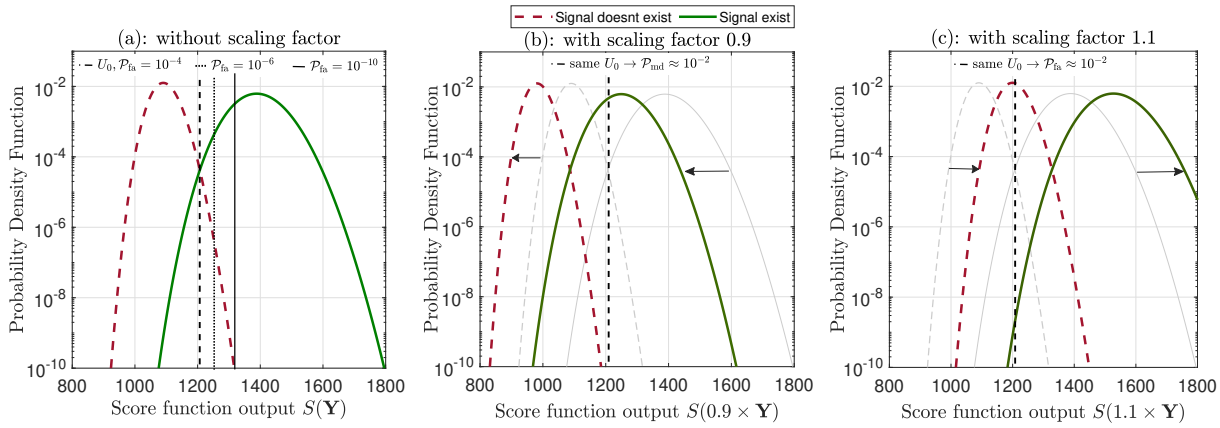

Fig. 2. Illustration of the detection problem and the effect of the scaling factor on threshold non-normalized detection probabilities.

and the associated correlation value is denoted γ_n, and given as

$$\gamma_n = L_n(d_n). \tag{6}$$

When the decision is correct ($d_n = c_n$), the expression of $\gamma_n = L_n(c_n)$ can be determined thanks to (2) and (3) as (see [8] for the details of the computation)

$$\gamma_n = e^{j\phi} e^{j(2\pi q f_0)n} q A(f_0) + Z_n. \tag{7}$$

with Z_n corresponding to the sum of the q samples of noise, i.e., a noise of variance $q\sigma^2$, ϕ given as $\phi = \varphi + \pi f_0(q-1)$ and $A(f_0) = \frac{\sin(\pi f_0 q)}{q \sin(\pi f_0)}$ the attenuation factor depending on f_0 ($A(f_0) \leq 1$, with $A(0) = 1$). One can note that when $f_0 = 0$, (7) gives $\gamma_n = e^{j\varphi} q + Z_n$. When $f_0 \neq 0$, in the absence of noise, the vector $\boldsymbol{\gamma} = (\gamma_n)_{n=0,1,\ldots,N-1}$ is a pure sinusoidal signal with a frequency of qf_0 (i.e. rotation of $2\pi q f_0$ radian between two consecutive components). This rotation prevents the coherent summation of the elements of the vector $\boldsymbol{\gamma}$. Therefore, the score function is obtained through a detection filter $S(\mathbf{Y})$ using incoherent summation, i.e., the summation of absolute values of γ_n.

$$S(\mathbf{Y}) = \sum_{n=0}^{N-1} |\gamma_n|. \tag{8}$$

The detector can determine whether a frame is present or not by comparing the value of the score function $S(\mathbf{Y})$ with a threshold U_0 in order to know the DET probabilities, i.e. probabilities of miss detection $\mathcal{P}_{md}$ and false alarm $\mathcal{P}_{fa}$. If the value of the score function exceeds the threshold U_0, the arrival of a new frame is assumed. However, if the value of the score function is lower than the threshold value, then the absence of a new frame is assumed. This first method of detection [8] is called the Incoherent Sum (IS) detection in the sequel.

Fig. 2(a) illustrates three different threshold values that correspond to various probabilities of false alarm $\mathcal{P}_{fa} = 10^{-4}, 10^{-6}$ and 10^{-10} versus the output of the correlation filter over a Gaussian channel. It can be clearly inferred from Fig. 2(a) that the threshold value U_0 allows a trade-off between $\mathcal{P}_{fa}$ and $\mathcal{P}_{md}$. In fact, in a perfect detection, both should be equal to zero to decide perfectly the presence or not of a new frame. In practice, the high value of U_0 decreases $\mathcal{P}_{fa}$ but increases $\mathcal{P}_{md}$, while the low value of U_0 has the symmetrical effect. For example, at threshold value $U_0 = 1200$ that corresponds to $\mathcal{P}_{fa} = 10^{-4}$, the probability of miss detection is approximately $\mathcal{P}_{md} = 10^{-4}$. This value increases to $\mathcal{P}_{md} = 5 \times 10^{-3}$ for U_0 corresponding to $\mathcal{P}_{fa} = 10^{-10}$. Thus, the value of U_0 is selected according to the system requirements.

B. Problem statement

The IS detection method proposed in [8] is efficient. However, it suffers from a flaw when the signal is affected by an unknown scaling factor. In fact, when the multiplicative factor is lower than expected, the miss detection errors increase. Fig. 2(b) shows the impact of a multiplicative factor of the received signal by a factor of 0.9. All the probability density functions are shifted to the left and, for a fixed threshold value, $\mathcal{P}_{md}$ increases by two decades. Fig. 2(c) illustrates the increase of false alarms for a multiplicative factor greater than 1. To mitigate this problem, [9] proposes to normalize γ_n in (8) by the norm $||\boldsymbol{y}_n||$ of $\boldsymbol{y}_n$ given by

$$\|\boldsymbol{y}_n\| = \sqrt{\sum_{l=0}^{q-1} |y_n(l)|^2} \tag{9}$$

to get the scaling factor invariant $\bar{\gamma}$ given as

$$\bar{\gamma}_n = \frac{\gamma_n}{\|\boldsymbol{y}_n\|} \tag{10}$$

Consequently, the new normalized score $\bar{S}(\mathbf{Y})$ is given as

$$\bar{S}(\mathbf{Y}) = \sum_{n=0}^{N-1} |\bar{\gamma}_n|. \tag{11}$$

This method is called Normalized Incoherent Sum (NIS) detection, since the summation is done on the module of $|\bar{\gamma}_n|$.

In the next section, we extend the NIS detection method to a Weighted Coherent Sum (WCS) detection. Then, the

combination of the two methods is performed in order to further improve the detection performance.

III. Weighted Coherent Detection

Let us first consider a Genius-Aided detector that knows perfectly the frequency offset f_0 and the N symbols c_n of the received frame. In this case, the optimal detection algorithm can be performed coherently, which increases greatly its performance. After describing the optimal Genius-Aided detector, we show how to take into account the fact that the transmitted symbols are unknown at the receiver side, but only estimated [9]. Then, we show how the FFT allows testing, with a low complexity cost, several frequency hypotheses in parallel to mitigate the fact that f_0 is also unknown. The resulting detector is called "Weighted Coherent Detection". Finally, the state-of-the-art detector [9] and the proposed WCS detector are combined to further improve the detection performance.

A. Genius-Aided detector

Assuming that the receiver knows the exact value of f_0, the residual frequency offset that affects the received symbol (see (1)) can be suppressed by multiplying $y(k)$ by $e^{-2j\pi f_0 k}$ prior to the computation of the $\boldsymbol{L}_n$. In that case, by taking d_n as c_n (known by the Genius), γ_n becomes equal to $qe^{2j\pi\varphi} + Z_n$, with $qe^{2j\pi\varphi}$ the coherent sum on q terms of the initial phase of the received signal and Z_n a Gaussian noise of variance $q\sigma^2$ (the sum of q independent noise of variance σ^2). The Genius-Aided score $\dot{S}_{GA}(\boldsymbol{Y})$ is given as

$$\dot{S}_{GA}(\boldsymbol{Y}) = |\sum_{n=0}^{q-1} \bar{\gamma}_n|. \tag{12}$$

During the coherent summation of the terms $\bar{\gamma}_n$, all the signal terms are added coherently, while the noisy terms are added incoherently. This leads to a high capacity to discriminate the hypothesis about the arrival, or not, of a frame.

B. CCSK Weighting factor

In this section, we will assume a Partially Genius-Aided decoder (PGA-decoder) for which only f_0 is known by the receiver. In this case, the direct summation of the normalized $\bar{\gamma}_n$ values can be severely affected by the erroneous decision taken at the symbol level. In fact, when $d_c \neq c_n$, the amplitude of $\bar{\gamma}_n$ is high (at least, higher than $|L_n(c_n)|\|\boldsymbol{y}_n\|$) and the phase is not correlated with the true phase of $L_n(c_n)$. At low SNRs, where the detection method is a critical problem, the coherent summation of the normalized $\bar{\gamma}_n$ values gives a detection performance significantly inferior to detection based on the score function given in (8). To mitigate this problem, we propose to weight the $\bar{\gamma}_n$ by the reliability of the decision d_n before making the coherent summation. Our objective is to assign low weight to the $\bar{\gamma}_n$ associated with an unreliable decision, and high weight otherwise. To do so, we use the α_n weight defined as

$$\alpha_n = \frac{|\gamma_n| - |\epsilon_n|}{\|\boldsymbol{y}_n\|}, \tag{13}$$

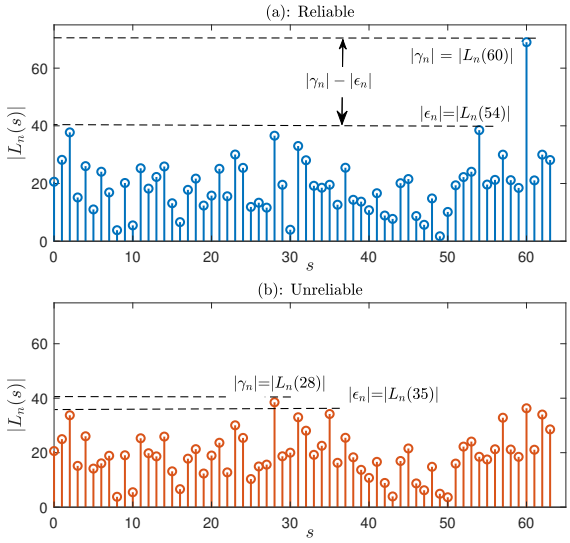

Fig. 3. CCSK weighting factor, a) case 1: reliable, b) case 2: unreliable.

where $|\epsilon_n|$ is the second maximum correlation value defined as

$$\epsilon_n = \max\{|L_n(s)|, s = 0, 1, \ldots, q-1, i \neq d_n\}. \tag{14}$$

The derivation of this weighted factor is obtained both with some mathematical arguments, not described here due to the lack of space (e.g. in a glance, it can be shown that Prob($d_c = c_n$) grows in $1/(1+ae^{-b\alpha})$, with a and b two constants), and by empirical experimentation. The normalization factor $\|\boldsymbol{y}_n\|$ of (13) is required to make the scaling factor α_n invariant to a scaling of the amplitude of the received frame $\boldsymbol{Y}$. Fig. 3 justifies graphically the link between α and the reliability of the decision d_n. In the upper plot, $|\epsilon_n| \ll |\gamma_n\|$ and the decision $d_n = 60$ is thus reliable. In the bottom plot, the correct decision is $d_n = 28$ but since $|\epsilon_n|$ is very close to $|\gamma_n|$, the correct decision could also be $d_n = 35$ with a significant probability.

The partially genius-aided score function $\dot{S}_{PGA}(\boldsymbol{Y})$ is thus given as

$$\dot{S}_{PGA}(\mathbf{Y}) = |\sum_{n=0}^{q-1} \alpha_n \bar{\gamma}_n|. \tag{15}$$

In the following section, we will consider that the frequency f_0 is unknown.

C. Frequency Domain Searching

The frequency offset f_0 is unknown. However, as explained earlier in the paper, f_0 is bounded between $[-f_m/2, f_m/2]$. It is thus possible to split this interval with a quantization step f_δ small enough so that coherent summation can be applied over the whole frame (more precisely, the whole vector $\bar{\gamma}$), typically $f_\delta \leq \frac{1}{4qN}$ so that the residual frequency error generates less than a quarter of rotation between γ_0 and γ_{N-1}. The most efficient way in testing all the hypotheses in parallel is to

compute the FFT $\mathbf{\Gamma}$ of the vector $\boldsymbol{\alpha} \cdot \bar{\boldsymbol{\gamma}} = (\alpha_n \bar{\gamma}_n)_{n=0,1,\ldots,N-1}$ with an FFT size L.

Let us study first the problem with almost ideal conditions, i.e., no noise ($Z_n = 0$, and no detection errors), $\bar{\gamma}_n = \gamma_n$ and $\alpha_n = 1$. Then, using the definition of the FFT of size L and the value of γ_n given in (7), we get

$$|\Gamma(i)| = |\sum_{n=0}^{N-1} \gamma_n e^{-j2\pi \frac{in}{L}}| \tag{16}$$

$$= A(f_0)q|\sum_{n=0}^{N-1} e^{j2\pi n(qf_0 - i/L)}|. \tag{17}$$

The maximum of $|\Gamma|$ is thus obtained for i_0 verifying $qf_0 - i_0/L = 0$. Taking into account that i_0 is an integer value, i_0 is rounded as $i_0 = \lfloor qf_0 L + 0.5 \rfloor$. Since by hypothesis, $f_0 \in [-f_m, f_m]$, then i takes its values inside the set $I = [\![-qf_m L, qf_m L]\!]$, or, taking into account the L periodicity of the FFT, i_0 takes its value inside the set $I = [\![0, qf_m L]\!] \cup [\![L(1-qf_m), L-1]\!]$. Finally, L should be high enough so that the $N(qf_0 - i_0/L) \ll 1$ in order for the summation of (17) remains almost coherent. In practice, we take $L = 4N$, which correspond to $f_\delta = 1/(4qN)$.

The WCS method is thus defined as

$$\begin{cases} \mathbf{\Gamma} = \mathcal{F}(\boldsymbol{\alpha} \cdot \bar{\boldsymbol{\gamma}}, L) \\ \dot{S}(\mathbf{Y}) = \max\{|\Gamma(i)|, i \in I\} \end{cases} \tag{18}$$

One should note that all the hypotheses used to justify the WCS detector are never verified in a real transmission. However, in spite of detection errors and noise, the score function $\dot{S}(\mathbf{Y})$ goes high enough in a presence of a frame to be used efficiently as a detection criterion, either alone, or combined with the NIS detector, as explained in the next chapter.

D. Joint NIS and WCS detector

The score function $\bar{S}(\boldsymbol{Y})$ given by the NIS method and $\dot{S}(\boldsymbol{Y})$ given by the WCS method are not fully correlated, as shown in Fig. 4 (note the ellipsoid shape).

It is thus possible to increase detection performance by using a linear combination of $\bar{S}(\mathbf{Y})$ and $\dot{S}(\mathbf{Y})$ by generating the new score function $\dot{\bar{S}}(\mathbf{Y})$ defined as

$$\dot{\bar{S}}(\boldsymbol{Y}) = \bar{S}(\boldsymbol{Y}) + m\dot{S}(\boldsymbol{Y}). \tag{19}$$

where m is a parameter that gives the slope of the line that separates the two clusters. Its value is selected in order to minimize the probability of miss detection for a given probability of a false alarm. In Fig. 4, a frame of length $N = 120$ symbols over GF(64) is considered at an SNR of -12 dB. Each point corresponds to a couple $(\dot{S}(\boldsymbol{Y}), \bar{S}(\boldsymbol{Y}))$ obtained either in the absence of a frame (lower left cluster, with a red circle) or in the presence of a frame (upper-right cluster, with blue cross). Each cluster contains 10^5 points. The thresholds for a probability of false alarm $\mathcal{P}_{fa} = 10^{-5}$ are indicated respectively by the vertical line (WCS detector: $\dot{S}(\boldsymbol{Y}) = 73.53$), the horizontal line (NIS detector: $\bar{S}(\boldsymbol{Y}) = 17256$)

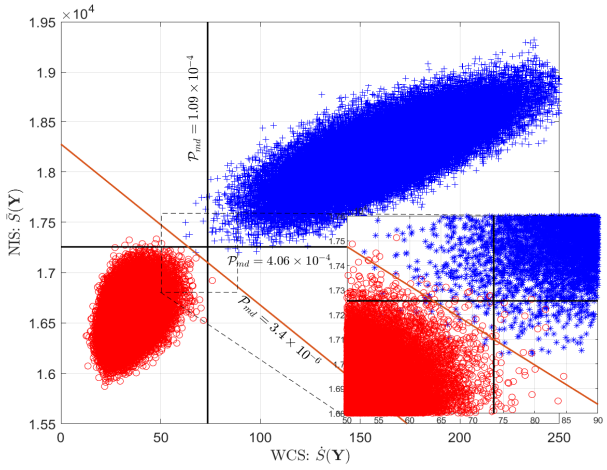

Fig. 4. Example of distribution of score functions of the NIS, WCS, and joint NIS-WCS detectors.

and the oblique line (joint WCS-NIS detector: $m = 16$ and $\dot{\bar{S}}(\boldsymbol{Y}) = 18175$). The zoomed region considers more points (5×10^6 instead of 10^5), to highlight the residual probability of miss-detection. In this example, we get $\mathcal{P}_{md} = 4.06 \times 10^{-4}$ for the NIS, $\mathcal{P}_{md} = 1.09 \times 10^{-6}$ for the WCS detector and $\mathcal{P}_{md} = 3.4 \times 10^{-6}$ for the joint NIS-WCS method, i.e. a reduction of more than two decades of $\mathcal{P}_{md}$ compared to the state-of-the-art NIS method.

IV. SIMULATION RESULTS

This section presents the simulation results of the proposed methods. Fig. 5 shows the DET probability curves for each detection method studied in this investigation, the considered

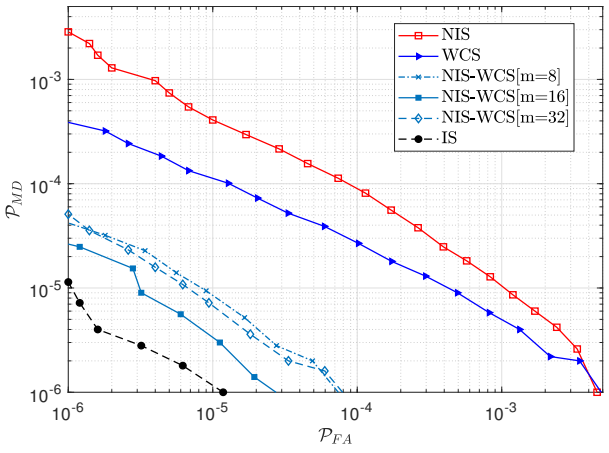

Fig. 5. DET probability curves, for a frame of $N = 120$ symbols in GF(64) for SNR $= -12$ dB, $n_0 = 0$, and $f_m = 1/(8q)$.

scenario is a frame of $N = 120$ symbols over GF(64) with a SNR of -12 dB, and $f_m = 1/(8q)$. First, it is observed that when using normalization (i.e., the NIS method), a noticeable degradation of the detection performance is observed

compared to the classical IS detector. This is due to the fact that the normalization factor canceled the side information given by the increase of energy when a frame arrives. This performance gap can be partially mitigated when using the proposed WCS method. However, the linear combination of NIS and WCS scores almost recover the performance gap. The DET probability curves are given for Several values of the slopes m. The optimal one is $m = 16$ (see also Fig. 4).

Under the same scenario, Fig. 6 shows the effect of the maximum offset frequency value f_m when using the classification technique with slope $m = 16$. When the value of

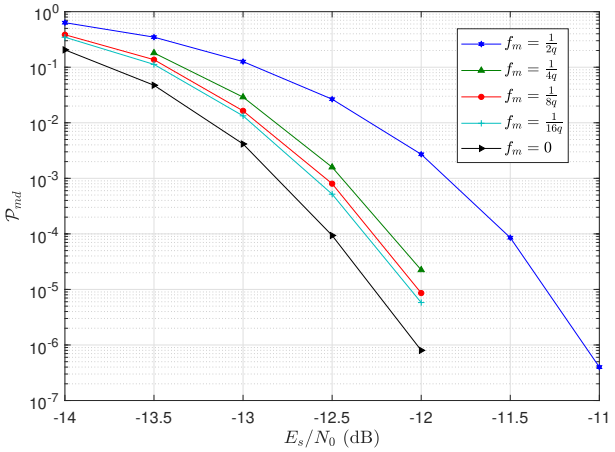

Fig. 6. $\mathcal{P}_{md}$ as a function of SNR for each offset frequency value f_m when using the classification technique ($m = 16$).

the maximum offset frequency amplitude f_m decreases, the detection performance becomes closer to the PGA decoder ($f_0 = 0$).

Finally, Fig. 7 shows the probability of miss-detection for a probability of false alarm $\mathcal{P}_{fa}$ of 10^{-5} for different detectors. The QCSP frame is of size $N = 120$ symbols over GF(64) and

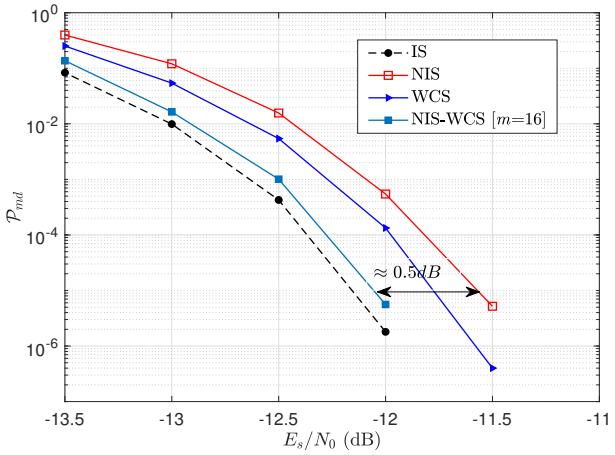

Fig. 7. $\mathcal{P}_{md}$ as function of E_s/N_0 for a QCSP frame of $N = 120$ symbols over GF(64) for $f_m = 1/(8q)$. The probability of false alarm $\mathcal{P}_{fa}$ is set to 10^{-5}.

the maximum absolute frequency offset is set to $f_m = 1/(8q)$. One can note in this figure that the proposed joint NIS-WCS detector is robust to scaling on the QCSP frame $\boldsymbol{Y}$, and just 0.1 dB below the detection performance of the IS detector for a probability of miss-detection of 10^{-5}.

V. CONCLUSION

This paper presents two contributions to improve the detection performance of a QCSP frame immune to a scaling factor on the input signal. The first contribution was to propose a detection method based on a weighted coherent sum of the decoded symbols. The second contribution was to combine linearly the score of the Normalized Incoherent Sum (from the state of the art) and the proposed Weighted Coherent Sum to further improve the detection performance. Compared to the state of the art, a gain of 0.5 dB of SNR has been observed (see Fig. 7). In the prospects, we will study intermediate solutions between the NIS and the WCS detectors. In fact, it is possible to do a coherent summation over each group of k consecutive decoded symbols and an incoherent summation over the N/k groups. We will also study the implementation of the proposed method in a real-time decoder.

REFERENCES

[1] G. Durisi, T. Koch, and P. Popovski, "Toward Massive, Ultrareliable, and Low-Latency Wireless Communication With Short Packets," *Proceedings of the IEEE*, vol. 104, no. 9, pp. 1711–1726, Sep. 2016.

[2] Y. Polyanskiy, "Asynchronous Communication: Exact Synchronization, Universality, and Dispersion," *IEEE Transactions on Information Theory*, vol. 59, no. 3, pp. 1256–1270, March 2013.

[3] D. Godard, "Self-Recovering Equalization and Carrier Tracking in Two-Dimensional Data Communication Systems," *IEEE Trans. Commun.*, vol. 28, pp. 1867–1875, 1980.

[4] K. M. Chugg and A. Polydoros, "MLSE for an unknown channel .I. Optimality considerations," *IEEE Transactions on Communications*, vol. 44, no. 7, pp. 836–846, 1996.

[5] T. Fujita, D. Uchida, Y. Fujino, O. Kagami, and K. Watanabe, "A burst modulation/demodulation method for short-packet wireless communication systems," in *2008 14th Asia-Pacific Conference on Communications*, 2008, pp. 1–5.

[6] B. Bloessl and F. Dressler, "mSync: Physical Layer Frame Synchronization Without Preamble Symbols," *IEEE Transactions on Mobile Computing*, vol. PP, pp. 1–1, 02 2018.

[7] P. Walk, P. Jung, B. Hassibi, and H. Jafarkhani, "MOCZ for Blind Short-Packet Communication: Practical Aspects," *IEEE Transactions on Wireless Communications*, vol. 19, no. 10, pp. 6675–6692, 2020.

[8] K. Saied, A. C. A. Ghouwayel, and E. Boutillon, "Short frame transmission at very low snr by associating ccsk modulation with nb-code," *IEEE Transactions on Wireless Communications*, vol. 21, no. 9, pp. 7194–7206, 2022.

[9] M. Camille, S. Kassem, L. G. Bertrand, and B. Emmanuel, "Time sliding window for the detection of ccsk frames," in *2021 IEEE Workshop on Signal Processing Systems (SiPS)*, 2021, pp. 99–104.

[10] K. Saied, A. Ghouwayel, and E. Boutillon, "Time-Synchronization of CCSK Short Frames," in *17th International Conference on Wireless and Mobile Computing, Networking and Communications (WiMob'2021)*, Bologna, Italy, Oct. 2021.

[11] K. Saied, A. C. A. Ghouwayel, and E. Boutillon, "Phase synchronization for non-binary coded ccsk short frames," in *2022 IEEE 95th Vehicular Technology Conference: (VTC2022-Spring)*, 2022, pp. 1–7.